Bacteria from Diverse Habitats Colonize and Compete in the Mouse Gut

Henning Seedorf,[1],[8] Nicholas W. Griffin,[1],[8] Vanessa K. Ridaura,[1] Alejandro Reyes,[1] Jiye Cheng,[1] Federico E. Rey,[1] Michelle I. Smith,[1] Gabriel M. Simon,[1] Rudolf H. Scheffrahn,[2] Dagmar Woebken,[3] Alfred M. Spormann,[3] William Van Treuren,[4] Luke K. Ursell,[4] Megan Pirrung,[4] Adam Robbins-Pianka,[4] Brandi L. Cantarel,[5] Vincent Lombard,[5],[6] Bernard Henrissat,[5],[6] Rob Knight,[4],[7] and Jeffrey I. Gordon[1],*

[1]Center for Genome Sciences and Systems Biology, Washington University School of Medicine, St. Louis, MO 63108, USA
[2]Fort Lauderdale Research and Education Center, University of Florida, Fort Lauderdale, FL 33314, USA
[3]Departments of Civil and Environmental Engineering and Chemical Engineering, Stanford University, Stanford, CA 94305, USA
[4]Biofrontiers Institute, University of Colorado, Boulder, Boulder, CO 80309, USA
[5]Centre National de la Recherche Scientifique, UMR 7257, 13288 Marseille, France
[6]Aix-Marseille Université, UMR 7257, 13288 Marseille, France
[7]Howard Hughes Medical Institute, University of Colorado, Boulder, Boulder, CO 80309, USA
[8]Co-first author
*Correspondence: jgordon@wustl.edu
http://dx.doi.org/10.1016/j.cell.2014.09.008

SUMMARY

To study how microbes establish themselves in a mammalian gut environment, we colonized germ-free mice with microbial communities from human, zebrafish, and termite guts, human skin and tongue, soil, and estuarine microbial mats. Bacteria from these foreign environments colonized and persisted in the mouse gut; their capacity to metabolize dietary and host carbohydrates and bile acids correlated with colonization success. Cohousing mice harboring these xenomicrobiota or a mouse cecal microbiota, along with germ-free "bystanders," revealed the success of particular bacterial taxa in invading guts with established communities and empty gut habitats. Unanticipated patterns of ecological succession were observed; for example, a soil-derived bacterium dominated even in the presence of bacteria from other gut communities (zebrafish and termite), and human-derived bacteria colonized germ-free bystander mice before mouse-derived organisms. This approach can be generalized to address a variety of mechanistic questions about succession, including succession in the context of microbiota-directed therapeutics.

INTRODUCTION

Understanding the factors that operate to allow microbes to colonize the human gut should help us achieve better understanding of how contact with other humans—including family members—animals, and other microbial reservoirs in our environment impacts diversity in this body habitat at various stages of life. This knowledge could also guide development of new approaches for modulating the risk for ecological invasion by various pathogens, deepen our understanding of how our microbial exposures shape the development of our immune systems, and help direct the design of more effective strategies for introducing members of well-defined species consortia, cultured from the gut microbiota of healthy donors, into already established microbial communities of recipient humans who are at risk for or already have manifest disease.

Macroecologists differentiate the conditions under which an organism can live (its fundamental niche) from the conditions in which the organism actually does live (its realized niche) (Hutchinson, 1957). Studies of macroecosystems have emphasized how a species' realized niche is often more restricted than its fundamental niche because negative interactions with other organisms prevent the species' successful colonization and persistence in areas in which it could live in their absence, or because historical, geographical, or physical processes have prevented that species from reaching certain areas. Colonization resistance, whereby established bacterial communities provide their hosts with some degree of protection against ecological invasion and overgrowth by pathogenic organisms, is a long recognized example of this phenomenon (Bohnhoff et al., 1964).

Gnotobiotic mice provide a powerful system for distinguishing the fundamental versus realized niches of microbes in the gut or other body habitats. Animals reared germ-free (GF) can be colonized at selected stages in their lives with control microbiota from conventionally raised mice or with alien microbiota (xeno-microbiota) harvested from the guts or other body habitats of other mammalian species, other vertebrates or invertebrates, or various highly divergent environmental habitats. A limited 16S rRNA-based analysis of reciprocal gut microbiota transplants involving conventionally raised mouse donors and GF zebrafish recipients, and conventionally raised zebrafish donors

and GF mouse recipients, demonstrated that bacterial taxa from zebrafish that had not been described in the normal mouse intestinal microbiota could persist in the mouse gut (Rawls et al., 2006): i.e., the mouse gut is within the fundamental niches of these microbes, but not in their realized niches. In this previous study, the gene repertoires represented in the gut-selected microbiomes were neither characterized nor were the relative abilities of the transplanted alien communities to invade the normal indigenous gut community of conventionally raised mice assessed.

In the present study, we extend this line of inquiry by identifying bacteria from a range of communities associated with different gut environments, other human body habitats, and aquatic and terrestrial environments, that successfully colonize the guts of GF mice. Furthermore, we compare the ability of these microbes to colonize empty gut habitats versus those with established microbial communities. The approach used should facilitate identification of successful gut colonizers that have therapeutic utility and the mechanisms that allow them to invade and persist.

RESULTS

Reproducibility of Xenomicrobiota Selection

We introduced microbiota from different habitats into separate groups of adult GF wild-type C57Bl/6J mice (five animals/cage; one gnotobiotic isolator/microbial community type; see stage 1 experiments in Figure 1). These xenomicrobiota included (1) gut-associated communities from a terrestrial vertebrate (human) and an aquatic vertebrate (zebrafish [*Danio rerio*]), plus an invertebrate (termite [*Nasutitermes corniger*]), (2) nongut communities from the same human donor (tongue and skin) so that the colonization success of taxa originating from human body habitats endowed with properties distinct from the gut could be ascertained, and (3) communities from the lower and upper layers of an estuarine microbial mat community and from a terrestrial (soil) community to assess the colonization potential of components of microbiota that reside in nonanimal habitats and contain many bacterial phyla not represented in the mouse gut (Harris et al., 2013; Tringe et al., 2005). Control "conventionalized" (CONV-D) animals received a cecal microbiota harvested from two adult conventionally raised, specific pathogen-free C57BL/6J mice that had been exposed to microbes in their vivarium since birth. Prior to and after transplantation, gnotobiotic mice were maintained on an autoclaved chow low in fat and high in plant polysaccharides ("LF-HPP diet"). Fecal samples were collected from transplant recipients over the course of the 28 days that followed gavage in order to (1) characterize the process of colonization and selection within and between the different groups of recipient animals, (2) determine whether a given community had achieved a stable composition during the period of surveillance, and (3) reference the results obtained from the xenomicrobiota recipients to the control group of CONV-D mice. (See Tables S1A–S1G [available online] for a list of samples characterized by multiplex pyrosequencing of PCR amplicons generated from variable region 2 [V2] of their bacterial 16S rRNA genes and Tables S1H–S1K for samples subjected to shotgun pyrosequencing of community DNA.)

Using the 16S rRNA data sets, we performed pairwise comparisons of communities employing UniFrac, a phylogenetic distance metric (Lozupone and Knight, 2005). Principal coordinates analysis (PCoA) of UniFrac distances revealed that all of the different types of transplanted communities assembled within recipient gnotobiotic mice over the course of 3–7 days and that the temporal pattern of assembly was very consistent within groups of mice that received the same input microbiota. UniFrac, as well as network analysis of shared operational taxonomic units (OTUs; each defined based on grouping of 16S rRNA reads with 97% nucleotide sequence identity [97%ID]), indicated that fecal communities from gnotobiotic mice that received vertebrate gut-derived microbiota generally were more similar to their respective input communities than to those originating from other sources (Figure 2; Figure S1).

To further test the reproducibility of community selection, we transferred the cecal contents of mice from stage 1, sacrificed 28 days after they had received their xenomicrobiota transplants, into a second group of age-matched GF male C57Bl/6J animals (see stage 2 in Figure 1). UniFrac distances between the original input communities and their corresponding stage 1 mouse-selected communities (day 14) were far greater than the distances between the selected stage 1 communities and the selected stage 2 communities (day 14) for all but the human fecal and control mouse cecal communities (Figure 2A). We also transplanted hindgut microbiota from two different colonies of termites and compared the output communities from stages 1 and 2. UniFrac distances were similar between selected termite communities across the two stages and between the two termite communities within a stage (Figure 2A), providing evidence of the reproducibility of the methods used for harvest (Potrikus and Breznak, 1977; Chen et al., 2012) and transplantation, as well as subsequent mouse gut selection of this notoriously fastidious collection of microorganisms.

Differences in the Diversity of Gut-Selected Xenomicrobiota

Bacterial communities selected from vertebrate and invertebrate gut microbiota maintained a significantly greater proportion of the taxonomic richness (97%ID OTUs), biodiversity (Shannon's diversity index), and evenness of relative abundance (Pielou's evenness index) relative to their input communities than did communities from nongut environments (soil; the upper layer, bottom layer, or mixed layers of the microbial mat; human tongue) (Figure S1E). This finding indicates that the mouse gut is within the fundamental niches of a greater proportion of bacterial taxa from other gut environments compared to taxa originating from other nongut habitats.

We identified a total of 1,908 97%ID OTUs in the input communities after rarefaction of the data (Extended Experimental Procedures). These OTUs spanned 76 different bacterial classes from 35 phyla. Most input communities shared very few or no OTUs with other input communities; Jaccard similarity values between input microbiota were zero for most pairs of communities and were higher for bacterial communities from similar sources (e.g., 0.57 for termite A and termite B; 0.31–0.41 for the microbial mat layers) (Figure S1B). This limited sharing of 97%ID OTUs was recapitulated in the recipient gnotobiotic
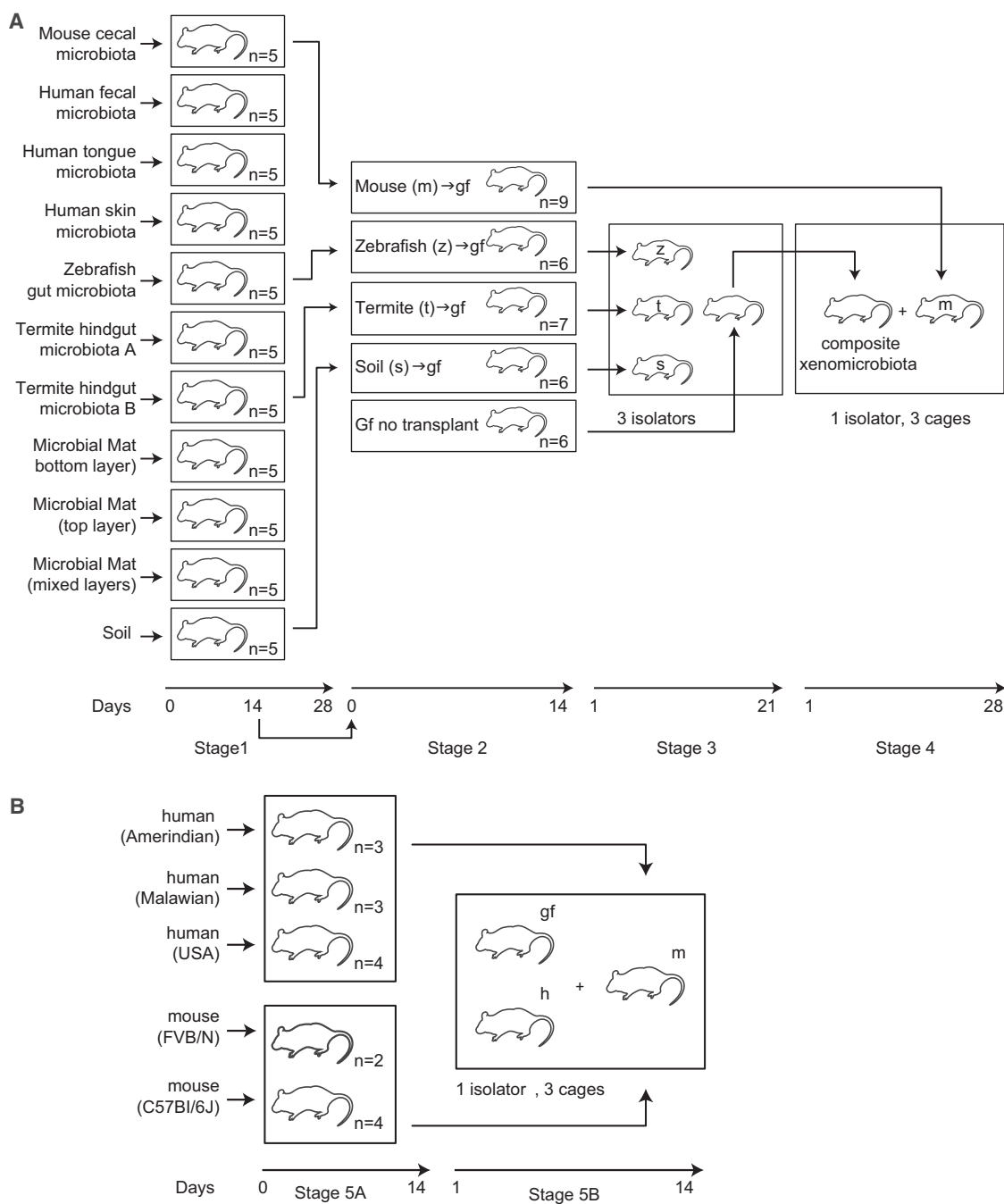
Figure 1. Design of Xenomicrobiota Transplant Experiments
(A and B) Summary of stages 1–5. See text for details. Abbreviations: m, mouse cecal microbiota; z, zebrafish gut microbiota; t, termite hindgut microbiota; s, soil.
Related to Table S1.

mouse gut-selected communities in which Jaccard similarities ranged from 0 to 0.33 and in which no OTUs were detected across all gut-selected communities.

Members of 15 bacterial classes from nine phyla established themselves in the mouse gut. Firmicutes was the only phylum represented in every selected community. This wide distribution of Firmicutes is consistent with a survey of the fecal microbiota of

mammals representing ten phylogenetic orders, three different gut physiologies (foregut fermenters, hindgut fermenters, and those with simple guts), and three different diet classes (herbivores, carnivores or omnivores; Ley et al., 2008; Muegge et al., 2011). Among the Firmicutes, Bacilli, and Clostridia were the most prominently represented classes (Figures 2B and S1A; see Tables S2A–S2K for a complete list of differences in the
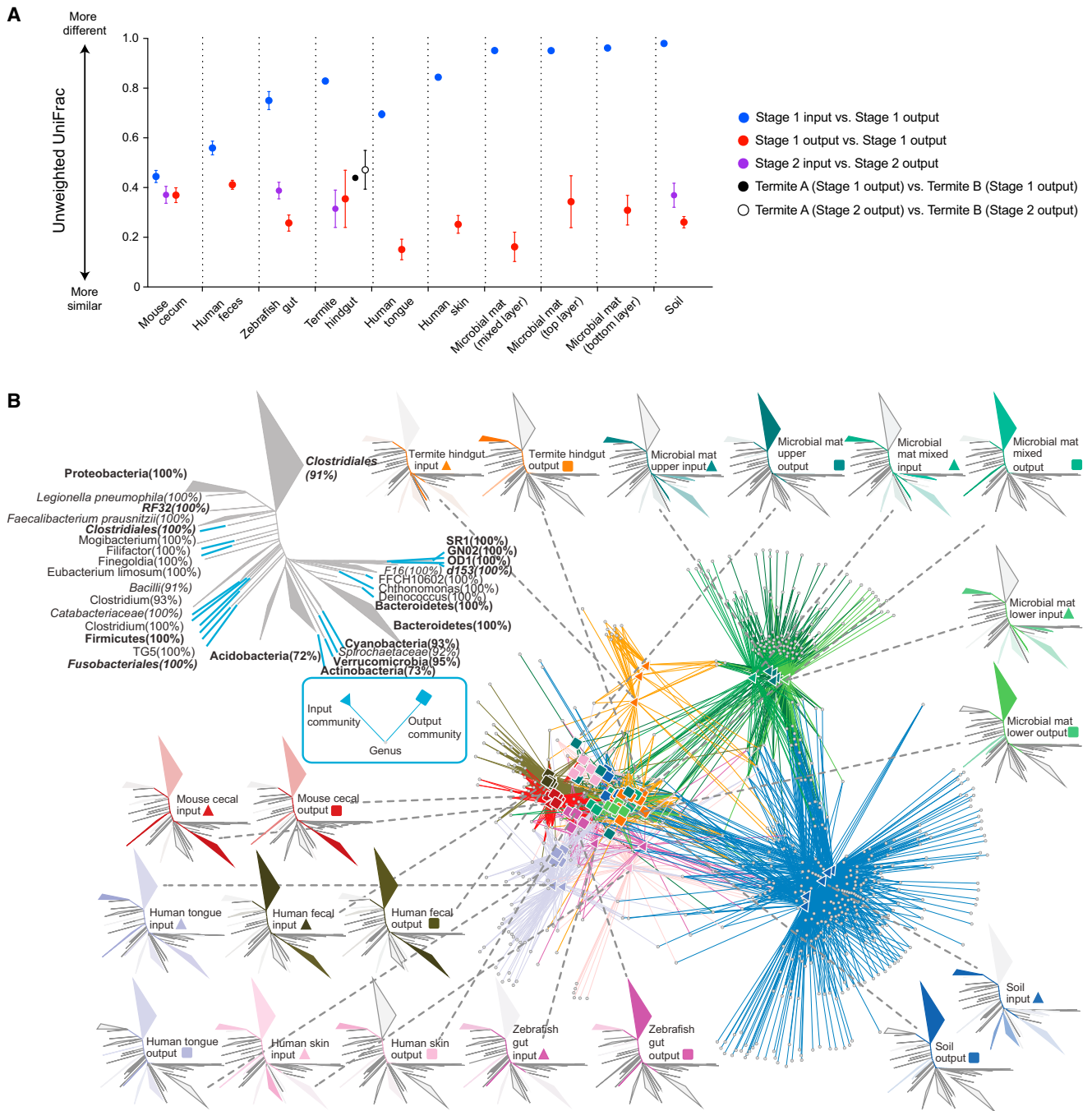
Figure 2. Comparison between Input Xenomicrobiota and Gut-Selected Communities in Gnotobiotic Mice from Stages 1 and 2

(A) Pairwise unweighted UniFrac distances. Abbreviations: input, input community introduced into mice by gavage; output, fecal samples collected from mice harboring transplanted microbiota. Mean values ± SD.

(B) Analysis of the fecal output communities collected from mice in the stage 1 transplant experiments shows that, despite the highly dissimilar input communities, the output communities cluster together, systematically excluding clades that fare poorly in the mouse gut. The large, gray phylogenetic tree in the upper left shows all of the 97%ID OTUs (collapsed into wedges at different taxonomical levels based on relative abundance) that are present in all samples collected from input and output communities. The numbers in parentheses next to each wedge indicate the percentage of the 97%ID OTUs collapsed into that wedge that were assigned to the specified taxonomy, i.e., 91% of the branches from the large clade at the top were assigned to the order Clostridiales, and 9% were assigned to other taxonomic groups. The smaller trees surrounding the network represent the input source (indicated by a triangle) and output fecal communities of mice (indicated by a square) at the end of stage 1 (28 days after gavage). All smaller phylogenetic trees are formatted identically to the schematic tree; therefore, each branch corresponds to the taxon indicated in the schematic. Each wedge is colored if taxa from that clade were present in the corresponding community. The

(legend continued on next page)

representation of bacterial genera detected in input compared to gut-selected output communities in stage 1 and stage 2 transplant experiments).

The Effects of the Adaptive Immune System, Diet, and Gastric Parietal Cell Ablation on Microbiota Selection

To examine the contribution of the adaptive immune system to selection of gut bacteria, adult GF male C57Bl/6J wild-type and $Rag1^{-/-}$ mice (which lack mature B and T cells) were colonized with the mouse cecal, zebrafish gut, and termite hindgut microbiota (n = 5 animals/treatment group). We used indicator species analysis to identify bacterial 97%ID OTUs that differed in their occurrence or relative abundances in $Rag1^{-/-}$ versus wild-type mice. Indicator species analysis uses indicator species values to measure the strength of association between an organism and a habitat type as the product of the organism's fidelity (probability of occurrence in a habitat type) and specificity (mean abundance in that type, normalized to the sum of its mean abundances in all other habitat types observed; Dufrêne and Legendre, 1997). A taxon is highly indicative of a particular habitat type if it is significantly more likely to occur in that type than in another or is much more abundant in that habitat. The significance of these associations was determined by permutation tests, followed by Benjamini-Hochberg corrections for multiple tests.

Indicator species analysis of fecal samples obtained at sacrifice 28 days after gavage revealed 29 97%ID OTUs that were differentially represented in $Rag1^{-/-}$ versus wild-type mice (p < 0.05; Table S3A). The most prominent effect of adaptive immune deficiency was observed in recipients of the native mouse gut (cecal) microbiota and was manifest by increased diversity of the selected community (see Table S3B for Shannon's diversity indices and the number of observed species; n = 23 differentially represented indicator OTUs, exemplified by OTU ID 230759 assigned to the genus *Allobaculum* whose relative abundance was 21.3% ± 4.0% [mean ± SEM] in wild-type recipients versus 7.2% ± 1.4% in $Rag1^{-/-}$ animals). Of the 29 OTUs identified as being differentially represented in immunodeficient compared to wild-type recipients, only seven were detectable in one but not in the other group (Table S3A). Together, these results suggest that the effects of adaptive immune deficiency on the diversity and representation of selected bacterial taxa originating from the two xenomicrobiota are less conspicuous than those observed with the autochthonous mouse gut microbiota because the selective pressures exerted on the xenomicrobiota upon transplantation into the "foreign" mouse gut environment are greater than those exerted by the adaptive immune system alone. (See the Extended Results; Tables S2L–S2R for a functional genomics analysis of transcriptional responses to colonization in the proximal colon, including responses related to the immune system.)

We examined the influence of diet by characterizing the effects of increasing the cellulose content of the chow on selection of 97%ID OTUs from the termite hindgut and the autochthonous mouse cecal microbiota (see the Extended Results; Tables S3C–S3J).

We also evaluated the effects of gastric acid on selection by colonizing GF *Atbp4-tox176* transgenic mice with a genetically engineered ablation of their parietal cells, and their nontransgenic littermates, with a fecal microbiota obtained from a healthy human donor. Compared to nontransgenic animals, *Atbp4-tox176* mice had no significant differences in Shannon diversity indices and in the number of observed bacterial 97%ID OTUs in their proximal small intestines, ceca, and colons or in their feces (sampled between days 22 and 42 after gavage). Significant differences in these indices were only observed in their gastric mucosa-associated microbiota (p < 0.001; one-way ANOVA, Šidák test for multiple hypothesis; Figures S2A and S2B). Comparisons of pairwise Hellinger distances revealed modest albeit statistically significant differences in community composition between the two groups of mice at all sites sampled, except in the proximal small intestinal mucosa (Figure S2C). These differences were attributable to just 16 OTUs, 15 of which belonged to the Firmicutes (Figures S2D–S2I). The results led us to conclude that gastric acid (and other parietal cell products) do not present a significant barrier to colonization of the distal mouse intestine by human gut taxa introduced via oral gavage.

Functional Properties of Selected Xenomicrobiota

We characterized the functional properties of the mouse gut-selected xenomicrobiota by measuring their biomass (productivity), defining their gene repertoires, and by profiling levels of various metabolites in cecal contents. The selected mouse cecal and human fecal communities had the highest and equivalent biomass (based on measurements of fecal DNA levels; Reyes et al., 2013), followed in descending order by the gut-selected soil, microbial mat, and termite hindgut communities. Selected communities from human skin, tongue, and zebrafish gut achieved the lowest biomass in recipient mice (Figure 3A).

Shotgun pyrosequencing reads generated from fecal community DNA were used to query the National Center for Biotechnology Information (NCBI) nonredundant database for taxonomic assignments (Tables S4A and S4B), the Kyoto Encyclopedia of Genes and Genomes for KEGG Orthology group (KO) and Enzyme Commission (EC) number assignments (Tables S4C and S4D), the Carbohydrate Active Enzymes (CAZy) database for glycoside hydrolase, polysaccharide lyase, carbohydrate esterase, and carbohydrate binding module family classifications, and the MEROPS database for peptidase families (Tables S4E and S4F). Reads collected from all gut-selected microbiomes were assigned to a total of 4,706 KOs, 1,621 ECs, 267 CAZyme families, and 479 peptidase families; 404 KOs

coloring for each tree is normalized to the relative abundance of OTUs for each source (i.e., darker colors represent taxa that were in higher relative abundance in a particular input or output community). Each phylogenetic tree is connected by a dashed line to the corresponding nodes within the network. In the network, the nodes represent genus-level OTUs and are connected by edges to either input communities (represented by triangles) or output communities (represented by squares) or to both. The network is constructed to minimize the spring forces over all nodes and therefore to bring communities sharing more genera together. Each community's nodes and edges in the network are uniquely colored to match their corresponding phylogenetic tree.
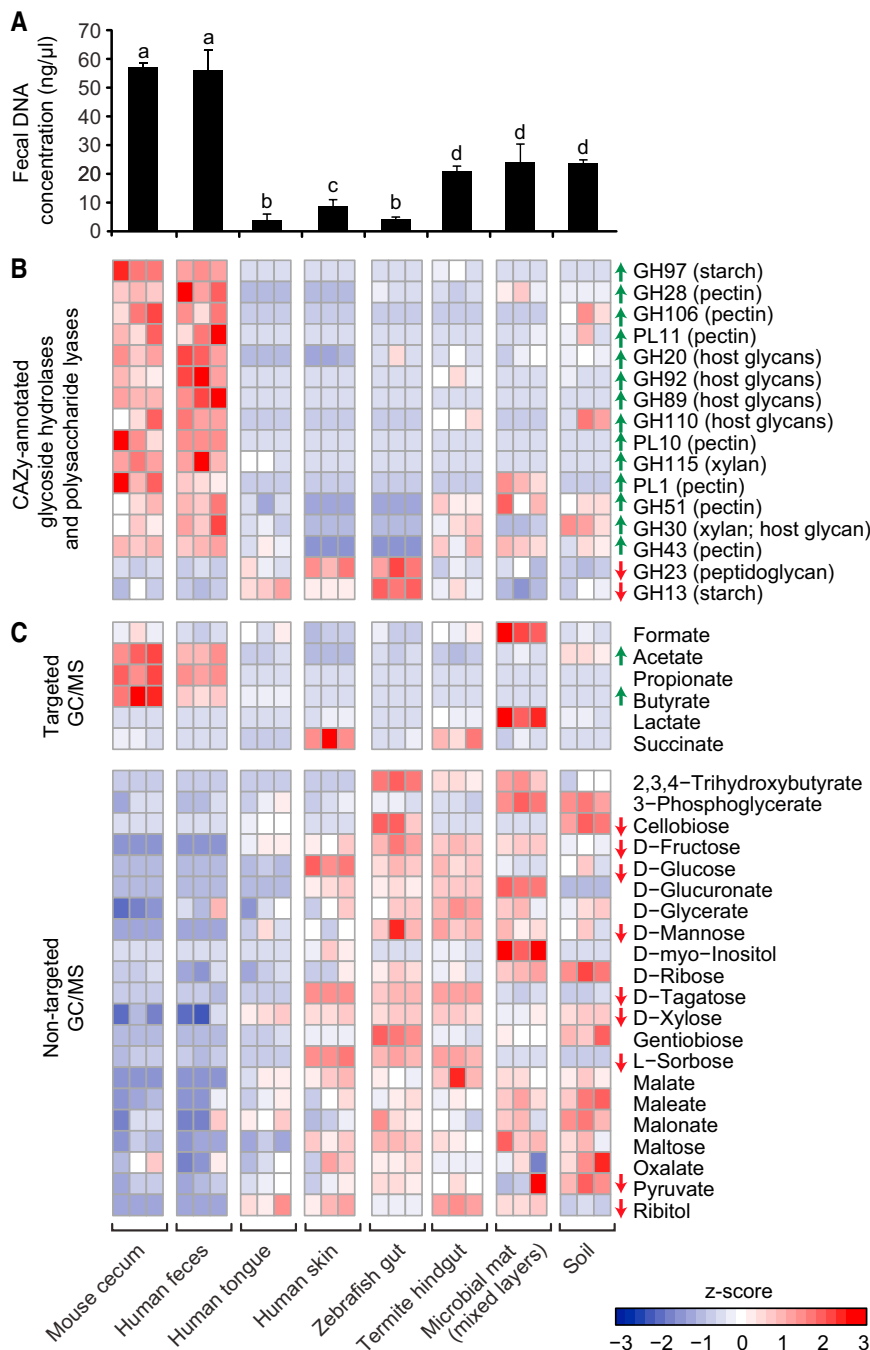See also Figures S1, S2, and S3 and Tables S2 and S3.

Figure 3. Correlations between Fecal Microbial Community Biomass and the Functional Properties of Selected Xenomicrobiota

(A) Fecal DNA concentrations (a proxy for microbial biomass) from mice harboring different microbiota, defined at the end of stage 1. Mean values ± SD are presented, with significant differences between bars denoted by different letters ($p < 0.05$; ANOVA; Tukey's correction for multiple hypotheses).

(B) Heatmap showing the normalized abundance (Z score) for CAZy-annotated glycoside hydrolases and polysaccharide lyases as determined by shotgun sequencing of stage 1 output fecal microbiomes sampled 28 days after gavage.

(C) Targeted and nontargeted GC-MS of the concentrations of SCFAs, carbohydrates, and other metabolites in cecal contents obtained at sacrifice from mice harboring the indicated selected microbiota. Arrows at the end of each row indicate if the CAZyme or metabolite is significantly positively (green arrow) or negatively (red arrow) correlated with fecal DNA concentration (Pearson's correlation, adjusted with Benjamini-Hochberg correction, $p < 0.05$).

See also Figures S3 and S5 and Tables S4 and S5.

community selection. CAZymes shared across the gut-selected microbiomes included eight glycoside hydrolase families, the most prominent being GH13 (includes α-amylases and pullulanases that breakdown starch, a universal storage polymer that is readily processed to glucose by virtually all animals and their associated microbiota, and three carbohydrate esterase families but no polysaccharide lyase families (see Figure 3B and Table S4I for CAZyme family abundances in different selected communities). The prominence of GH13 is consistent with the large amount of starch in the LF-HPP diet. Shared MEROPS families included aspartyl-, cysteinyl-, metallo-, and serine-peptidases (Table S4J).

Hellinger distance-based PCoA plots revealed a consistent pattern of similarity/dissimilarity among mouse gut-selected xenomicrobiomes. Termite and skin were most dissimilar to all others along the first principal coordinate (PC1). Among the others, three clusters were evident along PC2: zebrafish and tongue, soil and mat, and human and mouse gut microbiota.

Procrustes analysis disclosed that the goodness of fit between 16S rRNA data (97%ID OTUs summarized to the class level) and the representation of KOs, ECs, CAZymes, and MEROPS peptidases in the selected xenomicrobiomes was statistically significant, emphasizing the congruence of functional and phylogenetic characteristics (Figures S3A–S3D). (See Tables S4K–S4R

representing 314 ECs, 20 CAZyme family members, and 17 MEROPS peptidase family members were identified as being shared (Tables S4G–S4V). The observed number of shared CAZymes, ECs, KOs, and MEROPS families was significantly less than expected by chance alone (based on a test of 10,000 randomizations, $p < 10^{-4}$).

The CAZyme profile of the human microbiome varies between different human body habitats (Cantarel et al., 2012), suggesting that the local carbohydrate composition is a key driver for

for a summary of features that distinguish the selected xenomicrobiomes.)

Gut selection provided a "tool" for identifying previously unappreciated functional features present in the transplanted microbial communities. For example, hierarchical clustering of carbohydrate binding module (CBM) family members clearly differentiated selected xenomicrobiomes according to their host of origin in the LF-HPP diet context (Figure S4). Family AA10 (formerly classified as CBM33) consists of lytic polysaccharide mono-oxygenases (LPMOs; Hemsworth et al., 2013) that are of interest to the biofuels industry because they are able to open up the crystalline structure of recalcitrant polysaccharides, such as cellulose. AA10 genes were identified in all selected termite xenomicrobiomes (Figure S4; Table S4F); previous to this study, AA10 LPMOs had not been associated with the digestive tract of any animal species, including termites.

Fermentation of dietary polysaccharides, and putrefaction of proteins to amino acids with subsequent deamination and decarboxylation, produce short chain fatty acids (SCFAs) and gases (e.g., H_2). Targeted gas chromatography mass spectrometry (GC-MS) of cecal contents harvested from gnotobiotic mice at their time of sacrifice revealed that levels of acetate, propionate, and butyrate were highest in the selected mouse cecal and human fecal communities (Figures 3C and S5). Levels of these SCFAs were significantly correlated with microbial biomass (Pearson's correlation $r > 0.8$, $p < 0.001$). In contrast, formate, lactate, and succinate did not show significant correlations with fecal DNA levels. The relative abundances of genes encoding glycoside hydrolases (GH) and polysaccharide lyases (PL) were also significantly correlated with biomass (Pearson's $r = 0.48$, $p < 0.05$), the most highly correlated being members of families GH97, GH28, and GH106 (Table S4S; see Table S4T for correlations with MEROPS families). Measurements of 54 cecal metabolites by nontargeted GC-MS analysis revealed 11 (D-xylose, D-fructose, D-mannose, D-glucose, D-tagatose, L-sorbose, cellobiose, ribitol, and pyruvate, as well as cadaverine and 2-aminomalonate) with significant negative correlations with fecal DNA content (Pearson's $r < -0.5$, $p < 0.05$ after Benjamini-Hochberg correction; Table S5A; Figure 3C). Together, these results suggest that carbohydrate and protein degrading capacity are good predictors of community productivity/biomass in the gut. Moreover, Procrustes analysis disclosed that the goodness of fit between 16S rRNA data, the representation of ECs and the metabolite profiles was statistically significant (Figure S3E), further illustrating the congruence of functional and phylogenetic characteristics.

Conjugated bile acids produced by the host have microbicidal activities. Bacteria in the gut have evolved mechanisms for mitigating and modulating these effects, including expression of bile salt hydrolases (BSH) that catalyze deconjugation to primary bile acids (Jones et al., 2008) and hydroxysteroid dehydrogenases (HSDH) that transform primary to secondary bile acids. Postulating that xenomicrobiota with high biomass (productivity) phenotypes contain taxa that express these enzymatic activities, we used ultraperformance liquid chromatography-mass spectrometry (UPLC-MS) to measure the concentration of 34 bile acid species in fecal samples collected at the end of stage 2 from mice colonized with communities that achieved a range of biomasses (mouse cecal, soil, termite hindgut, and zebrafish gut microbiota). The results revealed a significant positive correlation between levels of deconjugated and secondary bile acid species and microbial biomass (Pearson's correlation, $p < 0.05$; $n = 6–8$ mice assayed/group; Figure 4A; Table S5B). The fact that this correlation occurs across communities suggests that increased deconjugation can lead to less microbicidal activity against selected allochthonous bacterial taxa, resulting in increased community biomass/productivity.

Ecological Invasion Assays

In a follow-up set of experiments (stage 3 in Figure 1), we tested the capacities of taxa comprising these different communities to compete for colonization of the mouse gut. Groups of four mice were cohoused: each tetrad consisted of one animal with a selected soil microbiota, one with a selected termite hindgut microbiota, another with selected zebrafish gut microbiota, and a GF "bystander" with no gut microbes. The cohousing setup was replicated in three separate cages, each placed in a different gnotobiotic isolator. Mice were surveyed over a 21-day period. Microbial SourceTracker (Knights et al., 2011) was used initially to analyze the effects of cohousing on the flow of microbes between cagemates. Fecal samples obtained from a given colonized mouse prior to cohousing were considered as "source communities." Cohoused animals exchange components of their gut microbiota via cophrophagy; therefore, fecal samples obtained during this period were considered as "sink communities." The experimental design allowed us to determine which organisms from the three gut-selected communities successfully invaded other communities and whether the assembly processes involved in shaping the communities in the colonized mice were replicated in the GF bystander.

Microbial SourceTracker and PCoA of unweighted UniFrac distances showed that cohousing led to rapid changes in the composition of the fecal microbiota of mice harboring the selected xenomicrobiota from stage 2 (Figures 5A and S6A). The fecal communities of all cagemates in all isolators converged to similar phylogenetic structures, dominated by organisms from the selected soil and zebrafish gut communities. The reproducible nature of these changes suggests that nonstochastic, selective processes played a role in shaping these communities.

We used indicator species analysis to identify the 97%ID OTUs that were most indicative of the selected stage 2 communities and tracked the success of these organisms during the course of the stage 3 cohousing experiments. To minimize the number of permutation tests performed in the indicator species analysis, and to ensure that we identified highly indicative 97%ID OTUs, we first removed those that did not occur in at least 75% of the mice harboring a given gut-selected microbiota type. Sharing of OTUs was rare between the different selected xenomicrobiota (mean Jaccard similarities ranged from 0.002 to 0.021); thus, it was not surprising that all of the 97%ID OTUs that met this conservative 75% threshold were subsequently identified as significant indicator taxa (see Table S6A for a complete list of these OTUs). We then tracked these indicator taxa derived from the mouse gut-selected soil, termite hindgut, and zebrafish gut as they colonized cohoused cagemates.
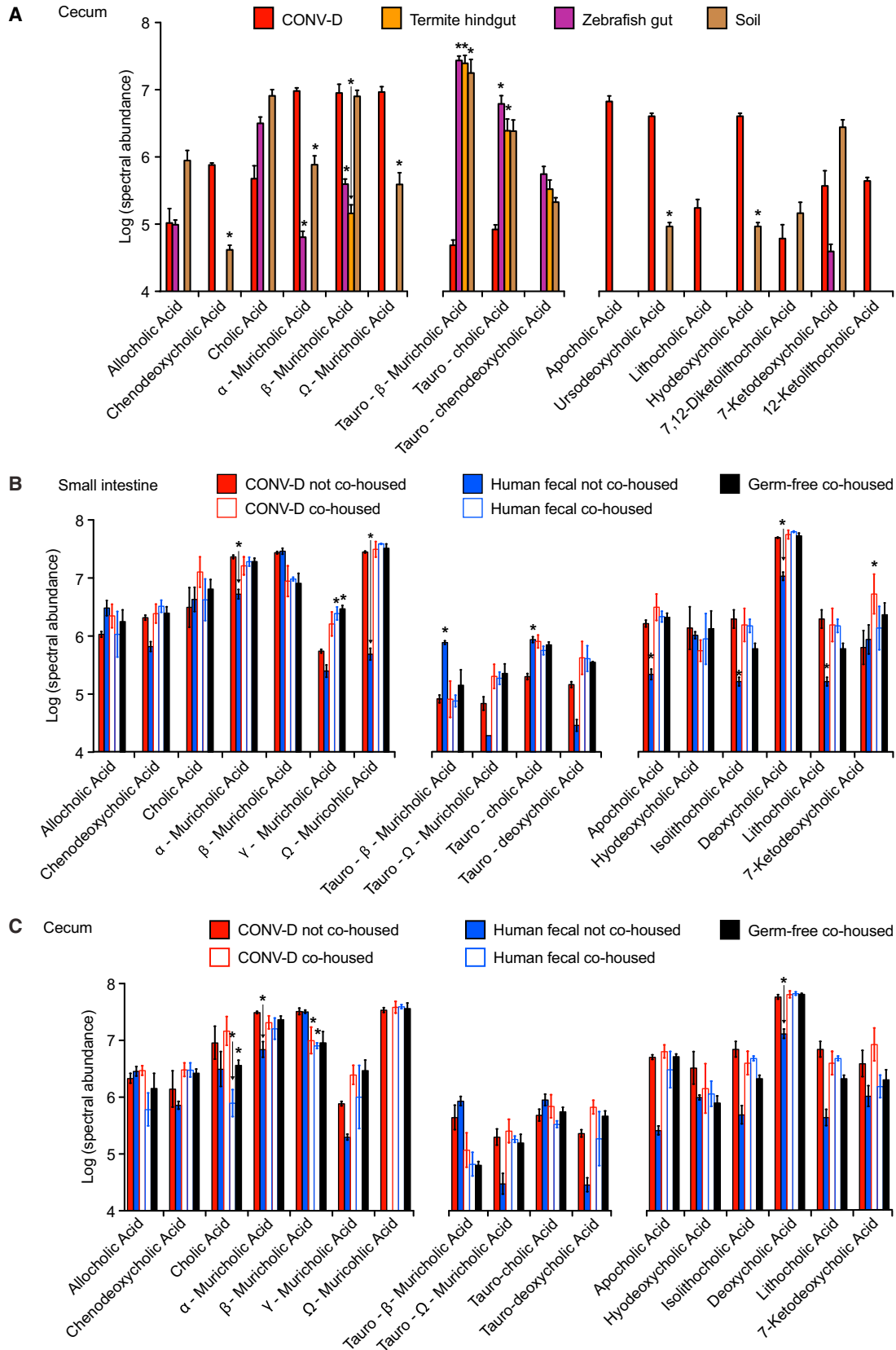
(legend on next page)

Within 1 day after initiation of cohousing in stage 3, the fecal communities of all cagemates (the GF bystander, plus mice originally colonized with the three different xenomicrobiota) were predominately composed of indicator OTUs belonging to Firmicutes derived from the mouse originally harboring the selected soil community and OTUs belonging to Firmicutes, Fusobacteria, and Proteobacteria from the cagemate originally colonized with the zebrafish community (Figures 5A and 5B). This pattern was consistent across all three gnotobiotic isolators. The highly successful zebrafish-derived Fusobacteria included members of the genus *Cetobacterium*. To date only two cultured species belonging to this genus, *Cetobacterium ceti* and *Cetobacterium somerae*, have been reported; the latter was recovered from the intestines of five freshwater fish species (Tsuchiya et al., 2008) and human feces (Finegold et al., 2003; Foster et al., 1995). This ecological invasion by *Cetobacterium* OTUs was followed by their marked reduction over the ensuing 7 days (Figure 5B). Termite hindgut-indicative 97%ID OTUs, including the dominant organism in the selected community (OTU ID 561718, assigned to *Enterobacter hormaechei*, Figure 5B), were initially detected in the guts of all cagemates, including the GF bystander, only to be largely extirpated at the end of 7 days of cohousing (Table S6A).

A single soil-indicative 97%ID OTU (OTU ID 169077; assigned to the phylum Firmicutes, family Lachnospiraceae, and genus *Ruminococcus* in the Greengenes reference 16S rRNA taxonomy [release 12_10]) achieved a relative level of abundance of 56.7% ± 4.0% (mean ± SEM) in all cagemates cohoused for 21 days in stage 3, a level comparable to that observed in mice harboring the selected soil xenomicrobiota in stages 1 and 2 (Figure 5B). Assembly of shotgun sequencing reads, generated from fecal or cecal samples that contained this very successful invasive opportunist, yielded a draft 7.2 Mbp genome (N50 contig length = 63,018 bp) containing 6,154 predicted protein-coding genes (Table S7A; Figures S7A and S7B). A single 16S rRNA gene sequence in the assembled contigs had 99.5% identity over 1,508 bp with an isolate of *Robinsoniella* (NCBI accession ID AF445283.2) and >99% identity to OTU ID 169077. The family Lachnospiraceae includes *Robinsoniella*, a genus with one previously described member that was recovered from swine and human feces (*Robinsoniella peoriensis*; Cotta et al., 2009; Gomez et al., 2011). Based on di-, tri-, and tetranucleotide frequencies in contigs >9.9 kb, this opportunist clustered with members of Lachnospiraceae and Clostridiaceae. Therefore, we designated the prominent soil xenomicrobiota-derived opportunist that came to dominate the guts of all cohoused cagemates in stage 3 experiments as *R. peoriensis.*

The KO, EC, and CAZyme content of our assembled *R. peoriensis* genome was compared to that of 150 sequenced human gut bacterial symbionts, representing a range of phylotypes (Table S7). The results revealed a notable enrichment for

CAZymes in the *R. peoriensis* opportunist, including 25 GH families predicted to breakdown host and plant-derived glycans (Z score > 2). The most enriched GH families (Z score > 8) included enzymes targeting host glycans (GH38 [α-mannosidase], GH98 [blood group A- and B-cleaving endo-β-1,4-galactosidases], GH111 [keratan sulfate hydrolase], GH123 [glycosphingolipid β-N-acetylgalactosaminidase], and GH125 [exo-α-1,6-mannosidase]) and one targeting plant carbohydrates (GH127; β-L-arabinofuranosidase) (Tables S7B and S7C). Moderately enriched families (Z score > 2 and < 8) included five other families involved in host glycan degradation (GH29 [α-L-fucosidase], GH33 [sialidase], GH95 [α-L-fucosidase], GH101 [endo-α-N-acetylgalactosaminidase], and GH112 [lacto-N-biose phosphorylase]) and several that process pectins (GH78 [α-L-rhamnosidase] and GH51 [α-xylosidase; α-L-arabinofuranosidase]) (Tables S7B and S7C). These results provide further support for the notion that realizing a niche within the distal guts of mice fed a LF-HPP diet is facilitated by a capacity to produce a broad range of CAZymes that target not only dietary but also host glycans.

Compared to the other 150 sequenced human gut bacterial strains, this opportunist is also enriched in (1) 15 MEROPS protease families, including a peptidase (M23.005) predicted to be a bacteriocin (zoocin A) involved in the breakdown of peptidoglycan, and S41.UNA (which could protect it from antibacterial peptides such as nisin; Table S7D), (2) a variety of ABC transporters, including those predicted to use maltose, Mg^{2+}, and heme as substrates (Table S7E), and (3) genes that support sporulation (a feature that could promote its survival outside the intestinal tract in soil; Table S7F). The assembled genome also contained two genes (RHS_0676 and RHS_1908) encoding protein products with significant similarity to nine predicted bile salt hydrolyases from the class Clostridia (which contains the genus *Robinsoniella*), and five genes (RHS_0652, RHS_1165, RHS_1257, RHS_2187, and RHS_4042) encoding proteins with significant homology to 18 Clostridial hydroxysteroid dehydrogenases (BLASTx, E-value $\leq 10^{-50}$) (Table S7G). This finding is consistent with the increased levels of fecal secondary bile acids documented in cohoused mice compared to mice colonized with just the zebrafish or termite hindgut communities.

In stage 4 experiments (Figure 1A), a formerly GF bystander mouse that had been exposed to three mice bearing the gut-selected soil, termite, and zebrafish communities from stage 3 ("composite xenomicrobiota" animal) was placed in a cage together with a CONV-D animal containing a transplanted mouse cecal gut microbiota. This cohousing scheme was replicated in three cages, each in its own gnotobiotic isolator. Applying Microbial SourceTracker and PCoA of UniFrac distances, we determined that there was rapid ecological invasion of the composite gut xenomicrobiota by members of the CONV-D mouse's gut

---

Figure 4. UPLC-MS of Bile Acids

(A) Analysis of cecal samples collected at the end of stage 2 from mice harboring selected xenomicrobiota from zebrafish gut, termite hindgut, or soil, and from CONV-D mice. *p < 0.05 compared to CONV-D animals, as measured by two-way ANOVA with Holm-Šidák correction for multiple hypotheses.

(B and C) Ileal (B) and cecal (C) bile acids from samples collected at the end of stage 5B from cohoused animals and from control noncohoused stage 5A mice harboring a selected composite human fecal xenomicrobiota or a composite microbiota from conventionally raised C57BL/6J and FVB/N mice (abbreviated CONV-D). Mean values ± SEM are presented. *p < 0.05 compared to CONV-D animals (two-way ANOVA with Holm-Šidák correction for multiple hypotheses). See also Tables S5C and S5D.
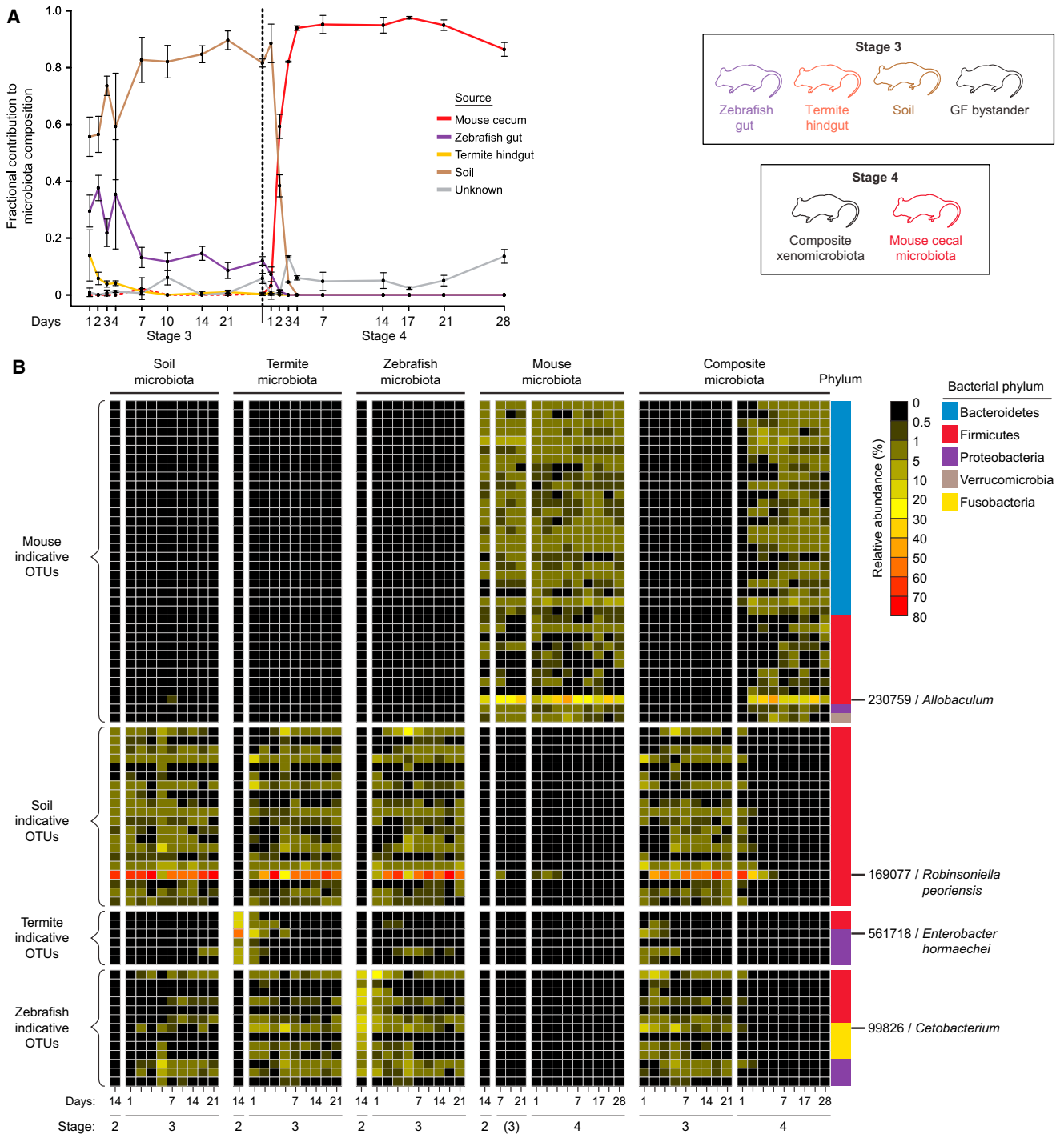
Figure 5. Analysis of Ecological Invasion in Stages 3 and 4 Cohousing Experiments

In stage 3 experiments, the GF mouse was cohoused with three mice transferred from stage 2: one with selected zebrafish gut xenomicrobiota, another with a selected termite hindgut xenomicrobiota, and a third with a selected soil community. During the stage 4 experiments, an ex-GF mouse from stage 3 that had acquired a composite xenomicrobiota was cohoused with a CONV-D mouse.

(A) The proportions of the different xenomicrobiota sources represented in the microbiota of the GF bystander over time defined using Microbial SourceTracker. Mean values ± SD are presented.

(B) Indicator species analysis identified bacterial 97%ID OTUs representative of the selected soil, termite hindgut, zebrafish hindgut, and mouse cecal microbiota at the end of stage 2. The heatmap shows the mean relative abundances of these OTUs in the fecal microbiota of each group of mice at each sampling time for

(legend continued on next page)

community (Table S6A); 10 days after initiation of cohousing, bacteria from the native mouse cecal community comprised >90% of the fecal microbiota of both cagemates across all three cages (Figures 5A and 5B; also see Figure S6A, which shows that the resulting communities cluster with those present in control noncohoused CONV-D mice).

We subsequently examined the behaviors of previously identified indicator OTUs throughout the stage 4 cohousing experiment. In mice harboring the composite xenomicrobiota, the soil- and zebrafish-indicative 97%ID OTUs that dominated communities in stages 2 and 3 experiments were largely replaced over the course of 4 days by mouse-associated OTUs (Figure 5B). The most abundant indicative 97%ID OTU in the fecal microbiota of the CONV-D cagemate prior to cohousing (OTU ID 230759 assigned to the genus *Allobaculum*) was the dominant invader of the composite xenomicrobiota. The *R. peoriensis* OTU, which dominated the composite xenomicrobiota in stage 3, remained detectable in these animals for up to 21 days after initiation of cohousing in the stage 4 experiments, but with a mean relative abundance of less than 0.1%. During the first 7 days of cohousing, 16 OTUs from the composite xenomicrobiota were able to invade the microbiota present in CONV-D animals. However, ecological invasion was short-lived; neither the *Robinsoniella* OTU nor any of the other 15 taxa were detected after 7 days (Figures 5B and S7C).

In a final transplantation experiment, one group of mice received human fecal microbiota samples from individuals representing three healthy adult human populations with distinct cultural traditions living on three continents (metropolitan areas of the United States, rural villages in southern Malawi, and the Amazonas state in Venezuela [Yatsunenko et al., 2012]; see stage 5A in Figure 1B and Table S1M). These animals were all cohoused to generate a composite human microbiota (n = 3–4 mice/donor microbiota placed in a single large cage in a single gnotobiotic isolator). The other group was colonized with microbiota harvested from conventionally raised C57Bl/6J or FVB/N mice (2–4 mice/microbiota; all recipient mice placed in a single large cage; Figure 1B) (Table S6B presents a list of 97%ID OTUs identified as human-indicative or mouse-indicative in these gut-selected communities). Fourteen days after receiving their microbiota transplants, a subset of the stage 5A animals were advanced to stage 5B. Stage 5B involved cohousing groups of three mice, one with a composite human gut microbiota, another with a composite mouse gut microbiota and a GF bystander, for 14 days (n = 3 cages of trio-housed animals; Figure 1B). Mice from stage 5A that were not cohoused were retained as controls. Microbial SourceTracker and indicator species analysis allowed us to follow the fates of human- and mouse-derived 97%ID OTUs during the course of stage 5B.

In the first days of cohousing in stage 5B, the fecal microbiota of GF bystanders were dominated by human-derived OTUs (Figure 6A); the most prominent belonged to the Peptostreptococcaceae and Erysipelotrichaceae, with members of the Bacteroida-

ceae and Lachnospiraceae families also well represented. By day 4, mouse-indicative taxa had begun to displace these human-indicative OTUs from the guts of the formerly GF bystander. This pattern of succession was characterized by the initial appearance of (1) members of two families in the Firmicutes (Lactobacillaceae [OTU 567604] and Erysipelotrichaceae [OTU 230759, the same *Allobaculum* OTU that became highly abundant in the guts of all cagemates in the stage 4 cohousing experiment]) and (2) a family in the Bacteroidetes (OTU 274749, assigned to family S24-7). These and other mouse-indicative taxa established themselves and became the dominant organisms (Figures 6A and 6D). Nonetheless, some human-indicative OTUs remained detectable at low abundances in these formerly GF cagemates even after 2 weeks of cohousing (e.g., two members of *Bacteroides*, OTU 311074 and 176794). In aggregate, these retained human indicator taxa represented 0.2% of the community at the end of the 14 day cohousing (see Table S6B for a complete list).

In cagemates that had originally harbored a selected human gut microbiota, the decay in relative abundances of human-derived taxa and the pattern of colonization by mouse-indicative OTUs mirrored the pattern observed in the GF bystanders (e.g., see OTU 230759 [genus *Allobaculum*] and OTU 274749 [family S24-7 in Figure 6D and Table S6B]). A small number of human-indicative taxa were also detectable in fecal samples harvested during and at the conclusion of the cohousing period from cagemates with the established composite mouse community (Table S6B); they comprised on average 0.5% of the fecal community of these mice and included OTU 311074 (assigned to the *Bacteroides*), which was also incorporated into the microbiota of the formerly GF cagemate.

These experiments paint a complex and unanticipated picture of ecological succession. Although OTUs originating from the mouse cecal microbiota came to dominate all cagemate gut communities after 2 weeks of cohousing (Figures 6 and S6B), the GF bystander allowed us to operationally define a group of human gut-derived taxa that exhibited a greater ability to colonize an unoccupied mouse gut than did microbes normally found in this habitat.

In mice, the primary bile acids are β-muricholic acid and cholic acid, whereas in humans they are chenodeoxycholic acid and cholic acid. Prior to their secretion into the biliary system, bile acids are conjugated in hepatocytes with either taurine (predominant in mice) or glycine (predominant in humans) to decrease their passive absorption by intestinal enterocytes (Hofmann et al., 2010; Vessey, 1978; He et al., 2003). UPLC-MS analysis of ileal and cecal contents revealed that mice colonized with the human fecal microbiota had different bile acid profiles than animals harboring the mouse microbiota. (1) The concentrations of deconjugated muricholic acids, most notably α- and Ω-muricholic acids, were significantly higher in the distal small intestines and ceca of animals with the mouse microbiota; (2) tauro-β-muricholic acid was significantly increased in the distal small intestine of

---

Stages 2–4. Note that a parenthesis is placed around stage 3 in the column labeled mouse microbiota to denote that this group of animals was advanced from stage 2 without subsequent cohousing during stage 3 (although sampled at the same times as cohoused stage 3 mice) and was subsequently used for the stage 4 cohousing experiments (see Figure 1A).

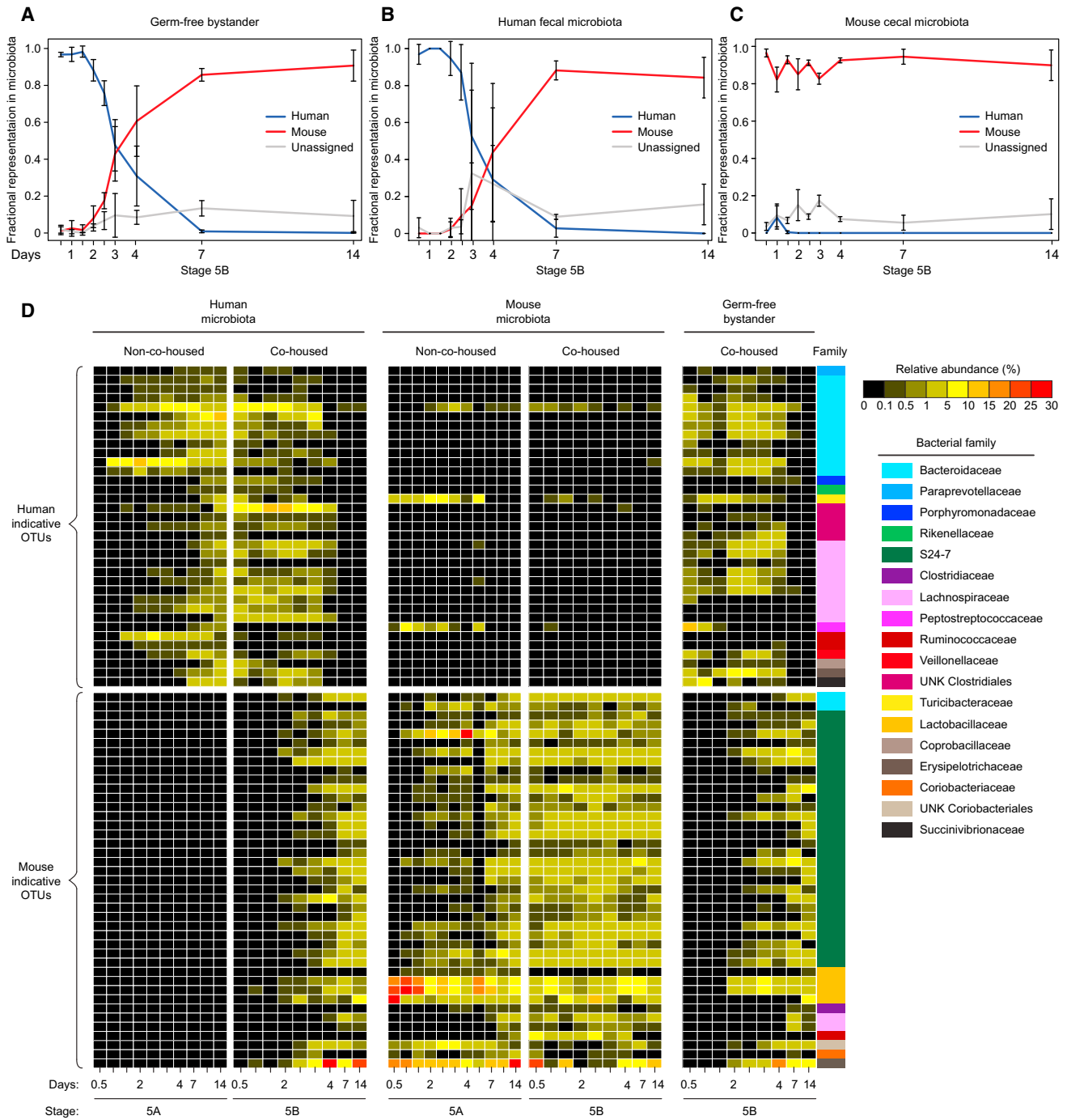See also Figures S6 and S7 and Tables S6A and S7.

Figure 6. Analysis of Ecological Invasion in Stage 5B Cohousing Experiments Involving Mice with Selected Composite Human Fecal Microbiota, a Composite Mouse Cecal Microbiota, and GF Bystanders

(A–C) Microbial SourceTracker was used to estimate the proportions of human-derived and mouse-derived bacteria (mean values ± SD) in (A) the GF bystander, (B) the mouse harboring a composite human fecal microbiota, and (C) the mouse harboring a composite mouse cecal community throughout the stage 5B cohousing experiment.

(D) The heatmap presents the mean percent relative abundances of mouse indicative and human indicative 97%ID OTUs in fecal samples collected from cagemates at the time points shown.

See also Figures S6 and S7 and Table S6.

mice colonized with the composite human fecal microbiota; and (3) levels of two secondary bile acids, isolithocholic acid and lithocholic acid, were significantly higher in the distal small intestines of animals with a composite mouse microbiota (Figures 4B and 4C; Tables S5C and S5D). At the conclusion of the stage 5B experiments, the microbiota of cagemates that had originally harbored a selected composite human fecal community contained levels of these bile acids that were now no longer significantly different from the composite mouse microbiota controls. (The originally GF bystander mice in the trio cohousing also had bile acid profiles indistinguishable from these controls.)

For further details, please refer to the Extended Results.

DISCUSSION

Our results indicate that the mouse intestinal tract, while highly selective, is within the fundamental niches of bacterial phylotypes derived from a wide variety of environments. Nonetheless, cohousing gnotobiotic mice with various selected xenomicrobiota together with CONV-D animals revealed that most bacterial phylotypes, including those selected from a human gut microbiota, are not capable of realizing a niche in a gut harboring an autochthonous microbiota.

Cohousing coprophagic gnotobiotic mice harboring different microbial communities together with GF bystanders provides a way to operationally define opportunists that can establish themselves in an uninhabited gut. It also provides a means for determining whether they can invade and persist within communities composed of microbes derived from any number of different sources. The success of these organisms can be correlated with functional features of the community and host; these correlations in turn generate hypotheses about previously unappreciated or unanticipated features of gut ecosystem properties.

Our experiments illustrate how the pattern of ecological succession in the gut cannot be solely predicted based on the habitat associations of organisms colonizing it. For example, trio cohousing experiments involving gnotobiotic animals harboring a mouse gut microbiota, a human gut microbiota, and GF bystanders, revealed human gut-derived taxa that colonized the GF bystanders before mouse-derived microbes did. Our correlational analyses yielded candidate functions that contribute to a taxon's ability to occupy the mouse gut (e.g., the ability to metabolize various carbohydrate substrates and host bile acids), at least in the context of the specific diet tested, and set the stage for future direct experimental tests of hypotheses generated from these cohousing experiments and similar experiments exploring a range of diets, stressor conditions, and genetic backgrounds. These tests may require development of tools for culturing and genetically manipulating identified prominent invaders and for more accurate modeling of microbial niches and resource utilization.

In the present study, we demonstrate the utility of this approach by using communities from vastly different environments. The approach can be generalized to address a variety of questions relevant to microbiota-directed therapeutics. Identifying beneficial and deleterious organisms, and the mechanisms that permit their successful colonization of the gut, will inform strategies for intentionally introducing or eradicating them. For example, cohousing experiments involving coprophagic, gnotobiotic mice that have received transplants of intact human fecal microbiota or sequenced collections of fecal bacteria from individuals representing healthy physiologic states and diseases of interest, represent the foundations of a preclinical pipeline for defining which components of different human microbiota can be exchanged and impact host biology (Ridaura et al., 2013; Faith et al., 2014). Creating such a pipeline for identifying next-generation probiotics is timely given the recent rapid expansion of efforts to treat humans with diseases ranging from *Clostridium difficile* colitis (Gough et al., 2011; Khoruts and Sadowsky, 2011; Hamilton et al., 2012) to metabolic syndrome (Vrieze et al., 2012) using fecal transplants, where uncertainties exist about formulating optimal criteria for donor and recipient selection, preparation, characterization, and administration of the donor sample, long-term effects, and safety.

EXPERIMENTAL PROCEDURES

Animal Husbandry

All experiments involving animals were performed using protocols approved by the Animal Studies Committee of Washington University. All human biospecimens were collected in accordance with procedures approved by the Washington University Human Research Protection Office.

Male C57Bl/6J wild-type and $Rag1^{-/-}$ mice (Jackson Laboratory) and FVB/N *Atbp4-tox176* transgenic mice (Syder et al., 1999) and their nontransgenic littermates were derived as GF and maintained in flexible plastic film isolators under a strict 12 hr light cycle (lights on at 0600). Unless indicated otherwise, animals were fed an autoclaved diet, low in fat and rich in plant polysaccharides (LF-HPP; B&K Universal) ad libitum. Mice received microbiota transplants at 8–12 weeks of age. Bedding was replaced in all experiments every 7 days.

Preparation of Xenomicrobiota for Transplantation

All microbiota samples were resuspended in filter-sterilized PBS (pH 7), supplemented with 2 mM dithiothreitol (DTT) in a Coy chamber containing an atmosphere of 75% N_2, 20% CO_2, and 5% H_2. Suspensions were transferred to a Balch tube that was then sealed. After transportation to the gnotobiotic mouse facility, the surface of the sealed Balch tube was sterilized by exposure to chlorine dioxide in the transfer sleave attached to the gnotobiotic isolator. Once imported into the isolator, a 200 μl aliquot of the suspension was removed from the tube and gavaged into GF recipient mice.

See the Extended Experimental Procedures for details about the sources of xenomicrobiota plus methods used for (1) isolation of DNA from input communities and from fecal and cecal samples collected from transplant recipients, (2) multiplex pyrosequencing of amplicons generated from the V2 region of bacterial 16S rRNA genes and multiplex shotgun pyrosequencing of community DNA plus analyses of the resulting data sets, (3) targeted and nontargeted GC-MS and UPLC-MS analyses of intestinal contents, and (4) functional genomic studies of host responses to the different xenomicrobiota.

ACCESSION NUMBERS

Bacterial 16S rRNA pyrosequencing data sets have been deposited in EMBL European Bioinformatics Institute (EBI) under the accession numbers ERP005633, ERP005634, ERP005636, and ERP005637. Shotgun pyrosequencing data sets of community DNA are available in EBI under the accession number ERP005635. GeneChip data have been deposited in Gene Expression Omnibus (GSE57589).

SUPPLEMENTAL INFORMATION

Supplemental Information includes Extended Experimental Procedures, Extended Results, seven figures, and seven tables and can be found with this article online at http://dx.doi.org/10.1016/j.cell.2014.09.008.

REFERENCES

Bohnhoff, M., Miller, C.P., and Martin, W.R. (1964). Resistance of the mouse's intestinal tract to experimental *Salmonella* infection. Factors responsible for its loss following streptomycin treatment. J. Exp. Med. *120*, 817–828.

Cantarel, B.L., Lombard, V., and Henrissat, B. (2012). Complex carbohydrate utilization by the healthy human microbiome. PLoS ONE *7*, e28742.

Chen, W., Wang, B., Hong, H., Yang, H., and Liu, S.J. (2012). Deinococcus reticulitermitis sp. nov., isolated from a termite gut. Int. J. Syst. Evol. Microbiol. *62*, 78–83.

Cotta, M.A., Whitehead, T.R., Falsen, E., Moore, E., and Lawson, P.A. (2009). *Robinsoniella peoriensis* gen. nov., sp. nov., isolated from a swine-manure storage pit and a human clinical source. Int. J. Syst. Evol. Microbiol. *59*, 150–155.

Dufrêne, M., and Legendre, P. (1997). Species assemblages and indicator species: the need for a flexible asymmetrical approach. Ecol. Monogr. *67*, 345–366.

Faith, J.J., Ahern, P.P., Ridaura, V.K., Cheng, J., and Gordon, J.I. (2014). Identifying gut microbe-host phenotype relationships using combinatorial communities in gnotobiotic mice. Sci Transl Med *6*, 220ra11.

Finegold, S.M., Vaisanen, M.L., Molitoris, D.R., Tomzynski, T.J., Song, Y., Liu, C., Collins, M.D., and Lawson, P.A. (2003). Cetobacterium somerae sp. nov. from human feces and emended description of the genus Cetobacterium. Syst. Appl. Microbiol. *26*, 177–181.

Foster, G., Ross, H.M., Naylor, R.D., Collins, M.D., Ramos, C.P., Fernandez Garayzabal, F., and Reid, R.J. (1995). *Cetobacterium ceti* gen. nov., sp. nov., a new gram-negative obligate anaerobe from sea mammals. Lett. Appl. Microbiol. *21*, 202–206.

Gomez, E., Gustafson, D.R., Colgrove, R., Ly, T., Santana, R., Rosenblatt, J.E., and Patel, R. (2011). Isolation of *Robinsoniella peoriensis* from four human specimens. J. Clin. Microbiol. *49*, 458–460.

Gough, E., Shaikh, H., and Manges, A.R. (2011). Systematic review of intestinal microbiota transplantation (fecal bacteriotherapy) for recurrent *Clostridium difficile* infection. Clin. Infect. Dis. *53*, 994–1002.

Hamilton, M.J., Weingarden, A.R., Sadowsky, M.J., and Khoruts, A. (2012). Standardized frozen preparation for transplantation of fecal microbiota for recurrent *Clostridium difficile* infection. Am. J. Gastroenterol. *107*, 761–767.

Harris, J.K., Caporaso, J.G., Walker, J.J., Spear, J.R., Gold, N.J., Robertson, C.E., Hugenholtz, P., Goodrich, J., McDonald, D., Knights, D., et al. (2013). Phylogenetic stratigraphy in the Guerrero Negro hypersaline microbial mat. ISME J. *7*, 50–60.

He, D., Barnes, S., and Falany, C.N. (2003). Rat liver bile acid CoA:amino acid N-acyltransferase: expression, characterization, and peroxisomal localization. J. Lipid Res. *44*, 2242–2249.

Hemsworth, G.R., Davies, G.J., and Walton, P.H. (2013). Recent insights into copper-containing lytic polysaccharide mono-oxygenases. Curr. Opin. Struct. Biol. *23*, 660–668.

Hofmann, A.F., Hagey, L.R., and Krasowski, M.D. (2010). Bile salts of vertebrates: structural variation and possible evolutionary significance. J. Lipid Res. *51*, 226–246.

Hutchinson, G.E. (1957). Concluding remarks. Cold Spring Harb. Symp. Quant. Biol. *22*, 415–427.

Jones, B.V., Begley, M., Hill, C., Gahan, C.G., and Marchesi, J.R. (2008). Functional and comparative metagenomic analysis of bile salt hydrolase activity in the human gut microbiome. Proc. Natl. Acad. Sci. USA *105*, 13580–13585.

Khoruts, A., and Sadowsky, M.J. (2011). Therapeutic transplantation of the distal gut microbiota. Mucosal Immunol. *4*, 4–7.

Knights, D., Kuczynski, J., Charlson, E.S., Zaneveld, J., Mozer, M.C., Collman, R.G., Bushman, F.D., Knight, R., and Kelley, S.T. (2011). Bayesian community-wide culture-independent microbial source tracking. Nat. Methods *8*, 761–763.

Ley, R.E., Hamady, M., Lozupone, C., Turnbaugh, P.J., Ramey, R.R., Bircher, J.S., Schlegel, M.L., Tucker, T.A., Schrenzel, M.D., Knight, R., and Gordon, J.I. (2008). Evolution of mammals and their gut microbes. Science *320*, 1647–1651.

Lozupone, C., and Knight, R. (2005). UniFrac: a new phylogenetic method for comparing microbial communities. Appl. Environ. Microbiol. *71*, 8228–8235.

Muegge, B.D., Kuczynski, J., Knights, D., Clemente, J.C., González, A., Fontana, L., Henrissat, B., Knight, R., and Gordon, J.I. (2011). Diet drives convergence in gut microbiome functions across mammalian phylogeny and within humans. Science *332*, 970–974.

Potrikus, C.J., and Breznak, J.A. (1977). Nitrogen-fixing Enterobacter agglomerans isolated from guts of wood-eating termites. Appl. Environ. Microbiol. *33*, 392–399.

Rawls, J.F., Mahowald, M.A., Ley, R.E., and Gordon, J.I. (2006). Reciprocal gut microbiota transplants from zebrafish and mice to germ-free recipients reveal host habitat selection. Cell *127*, 423–433.

Reyes, A., Wu, M., McNulty, N.P., Rohwer, F.L., and Gordon, J.I. (2013). Gnotobiotic mouse model of phage-bacterial host dynamics in the human gut. Proc. Natl. Acad. Sci. USA *110*, 20236–20241.

Ridaura, V.K., Faith, J.J., Rey, F.E., Cheng, J., Duncan, A.E., Kau, A.L., Griffin, N.W., Lombard, V., Henrissat, B., Bain, J.R., et al. (2013). Gut microbiota from twins discordant for obesity modulate metabolism in mice. Science *341*, 1241214.

Syder, A.J., Guruge, J.L., Li, Q., Hu, Y., Oleksiewicz, C.M., Lorenz, R.G., Karam, S.M., Falk, P.G., and Gordon, J.I. (1999). Helicobacter pylori attaches to NeuAc α 2,3Gal β 1,4 glycoconjugates produced in the stomach of transgenic mice lacking parietal cells. Mol. Cell *3*, 263–274.

Tringe, S.G., von Mering, C., Kobayashi, A., Salamov, A.A., Chen, K., Chang, H.W., Podar, M., Short, J.M., Mathur, E.J., Detter, J.C., et al. (2005). Comparative metagenomics of microbial communities. Science *308*, 554–557.

Tsuchiya, C., Sakata, T., and Sugita, H. (2008). Novel ecological niche of *Cetobacterium somerae*, an anaerobic bacterium in the intestinal tracts of freshwater fish. Lett. Appl. Microbiol. *46*, 43–48.

Vessey, D.A. (1978). The biochemical basis for the conjugation of bile acids with either glycine or taurine. Biochem. J. *174*, 621–626.

Vrieze, A., Van Nood, E., Holleman, F., Salojarvi, J., Kootte, R.S., Bartelsman, J.F., Dallinga-Thie, G.M., Ackermans, M.T., Serlie, M.J., Oozeer, R., et al. (2012). Transfer of intestinal microbiota from lean donors increases insulin sensitivity in individuals with metabolic syndrome. Gastroenterology *143*, 913–916.e7.

Yatsunenko, T., Rey, F.E., Manary, M.J., Trehan, I., Dominguez-Bello, M.G., Contreras, M., Magris, M., Hidalgo, G., Baldassano, R.N., Anokhin, A.P., et al. (2012). Human gut microbiome viewed across age and geography. Nature *486*, 222–227.